Do the spatial characteristics of myocardial scar tissue determine the risk of ventricular arrhythmias?

Ángel Arenal[1]*, Jesus Hernández[1], Esther Pérez-David[1], José L. Rubio-Guivernau[2], Maria J. Ledesma-Carbayo[2], and Francisco Fernández-Avilés[1]

[1]Hospital General Universitario Gregorio Marañón, Madrid; and [2]Universidad Politécnica de Madrid and CIBER-BBN, Madrid

Abstract   Sudden cardiac death is one of the main causes of mortality in patients with structural heart disease. Although an implantable cardioverter defibrillator significantly reduces the mortality rate, many patients never receive a shock. Identification of high-risk patients would reduce the costs associated with this therapy and prevent the deleterious effect of inappropriate discharges. As scar tissue is the substrate of ventricular arrhythmias in patients with structural heart disease, scar characterization could allow stratification of the risk. The objective of this article is to review the role of scar characteristics in the pathogenesis of ventricular arrhythmias in patients with structural heart disease.

Keywords   Myocardial scar • Ventricular tachycardia

This article is part of the Spotlight Issue on: Reducing the Impact of Myocardial Ischaemia/Reperfusion Injury

1. Introduction

Monomorphic ventricular tachycardia (MVT) in patients with structural heart disease can be caused by several mechanisms (e.g. bundle branch re-entry, fascicular re-entry, and automatism from cells located at the border of the scar or in the His–Purkinje system); however, most are caused by myocardial scar re-entry. Although myocardial scars can also appear during the evolution of right ventricular cardiomyopathy and congenital heart disease, this review examines the processes associated with left ventricular scars, namely ischaemic heart disease and non-ischaemic cardiomyopathy. In this article, in order to obtain accurate information on the scar dimension and heterogeneity of the scar, we will review the literature regarding the characteristics of the scar using three-dimensional (3D) navigation systems and contrast (gadolinium)-enhanced magnetic resonance imaging (ceMRI).

2. Ventricular tachycardia substrate in patients with ischaemic heart disease

2.1 Slow conduction determinants

2.1.1 Gap junction changes

The mechanism underlying sustained MVT in patients with chronic myocardial infarction is a re-entry in which the slow conduction pathways are composed of bundles of viable myocytes embedded in regional scars. These surviving myocytes join to create corridors that reach the border of the scar and connect to normal tissue.[1] The development of slow conduction pathways involves processes linked to cardiac remodelling, such as cardiac fibrosis,[2] which acts on surviving myocytes and leads to cell disconnection and zigzag conduction.[3,4] Cell connection depends on the integrity of gap junctions, which permit the passage of intracellular ions between cells. Gap junctions are formed by two connexons, one from each connected cell, which migrate from the Golgi apparatus to the intercalated disks and bind end to end with connexons from apposing cells. The factors affecting gap junctions and contributing to cell disconnection and formation of the anatomical substrate of ventricular arrhythmias are reduced expression of connexin (Cx) 43, which is commonly observed after myocardial infarction,[5] and misallocation of connexons. The turnover of gap junctions is very fast, because the half-life of Cx43 is as short as 2–5 h,[6] thus facilitating misallocation of a connexon in the membrane in patients with heart diseases such as myocardial infarction. The membrane signals that attract connexons to intercalated disks may be shifted to the lateral membrane, thus directing them towards the lateral non-disc sarcolemmal membrane.[7] Although these alterations in gap junction distribution may contribute to slow electrical conduction, their role is probably a minor one,

---

because conduction velocity slows only when Cx43 is reduced by 70–95%, but not by 50%.[8] This observation suggests that the reduction of Cx43 expression in patients with heart disease is probably not enough to reduce conduction velocity. In fact, deposition of collagen between myocytes may be required to slow conduction. A recent study suggested that only the synergism between sodium current reduction, along with increased fibrosis and impaired intercellular coupling, could lead to a marked decrease in conduction velocity.[9] Therefore, simply reducing gap junctions is not enough to slow conduction, and interaction between surviving myocytes and cardiac fibrosis seems to be necessary for the development of ventricular tachycardia (VT) substrate.

2.1.2 Fibroblasts and cardiac fibrosis

The heart is formed by different types of cells, mainly myocytes and fibroblasts.[10] In some species, fibroblasts account for more than half of all heart cells and produce the extracellular matrix (ECM), which is composed of several types of collagen, as well as fibronectin. The main role of the ECM is to create the scaffold for cardiomyocytes.[11] Cardiac fibroblasts and the ECM form a network to which the myocytes attach, and which helps to maintain the structural integrity of the heart while, at the same time, enabling fibroblasts to exert mechanical forces on the myocytes.[12] Cardiac fibroblasts are not isolated cells, because they can connect to other fibroblasts and myocytes by Cx45 and Cx43, as observed at homocellular and heterocellular junctions.[13,14] Mechanical stress and chemical signalling can activate cardiac fibroblasts after a cardiac injury, thus starting the remodelling process. The cardiac fibroblasts that, up to this point, have synthesized and degraded the ECM in such away that they have maintained a firm equilibrium, begin to increase the production of ECM that surrounds myocytes, thus disrupting cell connections, and generating electrical barriers that give rise to the discontinuous conduction that reduces conduction velocity.[15]

Remodelling not only implies an increase in ECM production, but also important changes in fibroblast phenotype. After heart injury, some fibroblasts express smooth muscle cell proteins that are not normally expressed in fibroblasts, such as α-smooth muscle actin. Fibroblasts with smooth muscle cell characteristics are called myofibroblasts.[16] This phenotype change has the following two importance consequences: (i) the contractile proteins that facilitate the healing process can also transmit mechanical tension to the myocytes; and (ii) myofibroblasts have higher Cx43 levels than fibroblasts, with the result that electrical coupling between isolated myocytes and myofibroblasts increases.[17] This observation is important, because contacts between fibroblasts and cardiomyocytes in intact and healthy hearts are weak.[18] Consequently, myofibroblasts have a significantly greater ability than fibroblasts to modify the electrophysiological characteristics of myocytes.

2.1.3 Effects of the interaction between myocytes and myofibroblasts

Myofibroblasts are present in post-infarction scars in humans. They have been found as early as 4–6 days after infarction, and seem to persist for many years.[19] As mentioned above, myofibroblasts can express Cx43 and Cx45, both among themselves and with cardiomyocytes. Consequently, the presence of these connexins enables electrical current to pass between myocytes and myofibroblasts. Although myofibroblasts do not express sodium channels, membrane resistance is so high that electrotonic current can flow between non-connected myocytes through fibroblast bridges over extended distances.[20] The electrical current flowing through connections between myocytes and fibroblasts causes a gradual decline in myocyte resting membrane potential, because fibroblasts are less polarized. Therefore, fibroblasts can partly depolarize myocytes into the range of sodium channel inactivation, thus producing slowing of conduction.[21] Myofibroblast contraction, which plays a key role in healing, may also cause slowing of conduction in scar areas after a myocardial infarction. Myofibroblasts can contract and transmit the contractile force to myocytes, thus activating mechanosensitive channels. The activation of mechanosensitive channels depolarizes the cardiomyocyte membrane and inactivates sodium channels.[22]

The above findings suggest the electro-anatomical interaction between surviving myocytes, fibrosis, and fibroblasts/myofibroblasts within the scar, which generates slow conduction pathways that form part of the re-entrant circuit. Therefore, characterization of the scar and the surviving myocytes could enable us to stratify the risk of arrhythmia after myocardial infarction.

2.2 Voltage mapping scar characteristics in patients with ventricular arrhythmias

As VT substrate is intimately related to surviving myocytes inside the scar, characterization of the VT substrate relies on identification of the scar. Scars are areas with few myocytes where fibrous tissue prevails; consequently, local electrograms recorded at these sites are characterized by lower voltage amplitude than electrograms recorded in normal tissue.[23] Scar areas can be identified according to the electrogram amplitude measured during catheter mapping, and delimited using navigation systems that permit the 3D reconstruction of the endocardial or epicardial surface of the cardiac chambers and project the voltage of the electrograms at the corresponding site on the surface. The resulting voltage maps can be visualized and analysed on a computer display. The voltage of the local electrogram is colour coded and can be adjusted according to different definitions of scar tissue (*Figure 1A*). Animal and human studies have identified the voltage cut-off that differentiates the electrograms recorded in normal and scar tissues.[24,25] A voltage >1.5 mV distinguishes normal myocardium from scar, and the scar itself can be differentiated into dense scar (≤0.5 mV) and scar border (>0.5 and ≤1.5 mV). These voltage limits have been used to establish a direct correlation between the extension of the scar in voltage maps and anatomical preparations.[24] Slow conduction areas within the scar are easily recognized during endocardial mapping by recording the electrograms with isolated components or late potentials (E-IC/LP).[26] IC and LP are components of the electrogram that are recorded beyond the end of the QRS and separated from the main component of the electrogram by an isoelectric line. Several studies have established the relationship between E-IC/LP and VT isthmuses.[26,27] IC/LP are not homogeneously dispersed around the scar, but located in specific areas. Around 70% of E-IC/LP form slow conduction channels (CC),[28,29] which are areas inside the scar that are differentiated from the surrounding scar by a higher voltage. These structures are easily identified in voltage maps by carefully adjusting the voltage threshold that defines the scar (*Figure 1B*).[28,29] This observation emphasizes a determinant characteristic of the scar, namely, the scar is not a homogeneous structure, but clearly a heterogeneous structure whose heterogeneity is related to surviving fibres. Therefore, heterogeneity is intimately related to arrhythmogenesis, as illustrated by ultrahigh-
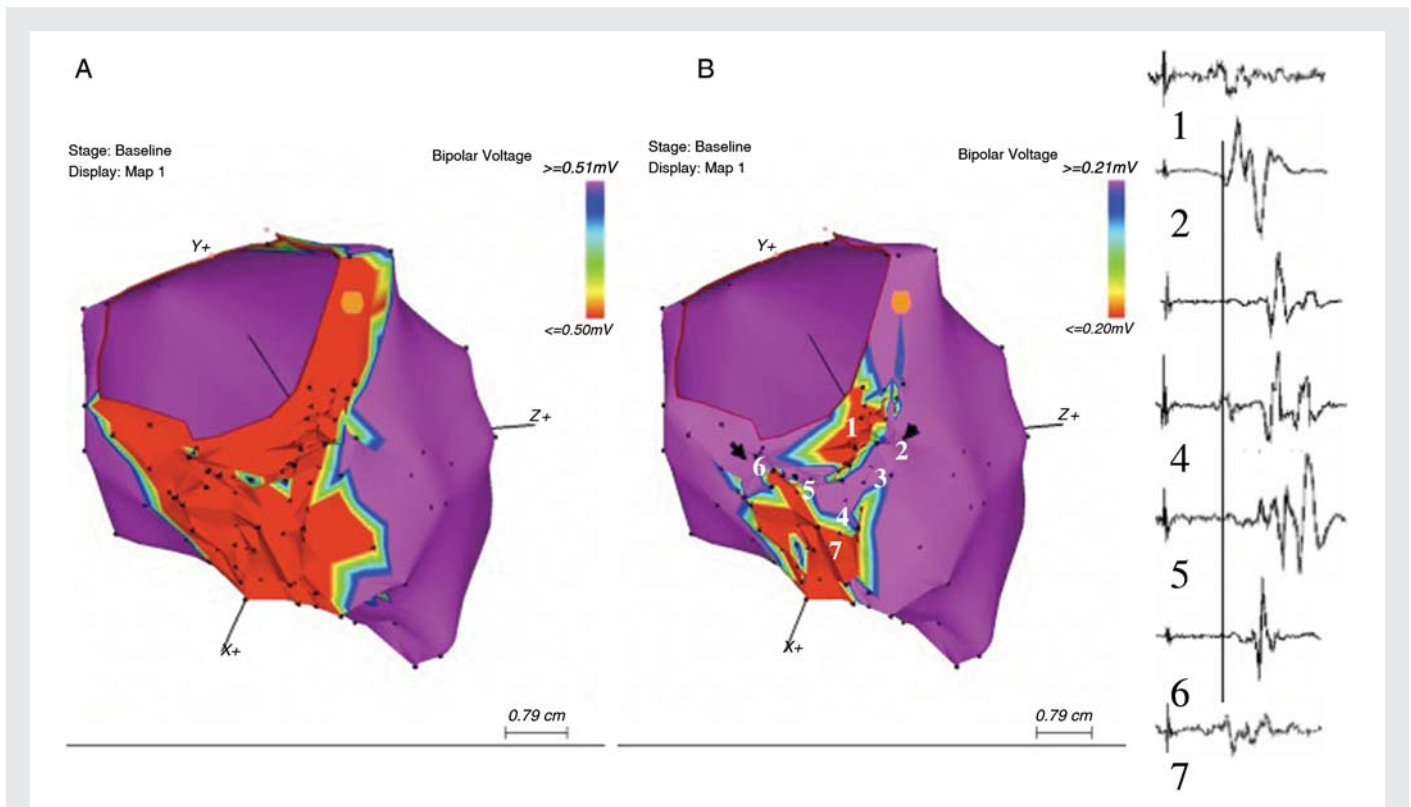
Figure 1 (*A*) Voltage map showing a scar in a patient with previous inferior myocardial infarction. The colour range represents the electrogram voltage amplitude. Dense scar is shown in red (electrogram amplitude ≤0.5 mV). (*B*) Voltage map showing the heterogeneity of the scar and conduction channels. This view of the inferior wall of the left ventricle shows a voltage map during right ventricular apical pacing, when the voltage that defined the scar was set at 0.2 mV. At this voltage, a channel spans from the septum to the lateral wall. The electrogram recorded at sites identified by white numbers is shown on the left of the panel. This figure shows the heterogeneous nature of the scar. Electrograms with a higher amplitude are inside the scar (electrograms 2−6); they usually present isolated components or late potentials (IC/LP), and are associated with the formation of conduction channels. Reproduced with permission from reference 28.

density mapping with multipolar catheters, showing that E-IC/LP that are critical to re-entry are adjacent to heterogeneous islets.[30] CC and E-IC/LP are sensitive and specific markers of VT substrate in ischaemic patients. Recent studies show that E-IC/LPs are found in more than 90% of VT isthmuses.[26,27,31] In addition, Haqqani *et al.*[32] reported that CC within dense scar tissue and adjacent to the mitral annulus and E-IC/LP were more frequently observed in sustained MVT patients than in control patients, despite similar left ventricle (LV) parameters, such as ejection fraction (EF).

These studies highlight an important finding, namely, that scar is not a homogeneous tissue, because some areas have a higher voltage owing to the presence of surviving fibres. These areas are corridors of slow conduction that can form part of re-entrant circuits. Therefore, ventricular arrhythmias are mainly due to scar heterogeneity.

2.3 Characterization of the scar by MRI

Contrast (gadolinium)-enhanced magnetic resonance imaging (ceMRI) can accurately identify and delimit myocardial infarction in both animals and humans.[33,34] Gadolinium is trapped by fibrous tissue, thus generating the higher signal intensity (SI) observed in MR images. In humans, an SI above 2 SD of the mean remote normal myocardium SI can be used to identify the infarct.[35] Signal intensity differentiates two areas within the scar: (i) the core area, defined by an SI >3 SD above the remote normal myocardium SI; and (ii) the

heterogeneous tissue (HT) or grey zone that contains the surviving myocytes mixed with fibrous tissue and that is defined by an SI of between 2 and 3 SDs[35] (*Figure 2*). The presence of viable myocytes causes the lower SI of the HT.

2.3.1 Scar characteristics and VT inducibility

Several studies have shown the association between non-invasively detected scar size and architecture and both inducible and spontaneous MVT. Bello *et al.*[34] reported that the infarct size and morphology detected by ceMRI is a better predictor of VT inducibility than LVEF. The authors studied 48 patients with known coronary artery disease who were referred for electrophysiological study using ceMRI. Scar characteristics were determined and compared between patients with no inducible VT, those with inducible MVT, and those with inducible ventricular fibrillation. Patients with MVT had larger infarcts than patients who did not have inducible arrhythmias. Patients with polymorphic VT/fibrillation had intermediate values. Logistic regression demonstrated that infarct mass and surface area were better predictors of inducibility of MVT than LVEF. Both size and characteristics of the scar are related to inducibility of MVT. Schmidt *et al.*[36] reported that HT mass detected by MRI was the best predictor of VT inducibility. VT inducibility was tested before implantation of an implantable cardioverter defibrillator (ICD) for primary prevention in 47 patients who underwent ceMRI. When inducible and non-inducible patients

Figure 2 Identification of scar, dense scar, and heterogeneous tissue based on measurement of signal intensity (SI) using contrast (gadolinium)-enhanced magnetic resonance imaging (ceMRI). This ceMRI long axis view shows the anteroseptal infarct as high SI (area inside the continuous line) and the normal myocardium as dark SI. Heterogeneous tissue was defined using the following process: (i) the endocardial and epicardial borders were drawn; and (ii) a region of interest in the remote non-infarcted myocardium and the normal SI was defined (site 2). The myocardial segment with an SI > 2 SD of the infarcted region was loosely outlined. Heterogeneous tissue (sites 3 and 4) can be differentiated inside the infarcted area (SI > 2 SD < 3 SD) and dense scar (SI>3 SD; site 5).

were compared, no differences were observed between LVEF, LV end-diastolic volume, and infarct size. Nevertheless, HT mass was significantly higher in inducible patients, and was the only significant predictor in stepwise logistic regression analysis.

2.3.2 Scar characteristics and prognosis after myocardial infarction

Not only is scar characterization useful for differentiating patients with inducible VT, it can also establish outcome after myocardial infarction. Yan et al.[35] studied 144 patients with documented coronary artery disease and abnormal myocardial delayed enhancement consistent with post-infarction scar. Based on the SI, the authors measured the total infarct size and divided it between the scar core and HT. After a median follow-up of 2.4 years, 29 (20%) patients died. Patients with an above-median HT/infarct size quotient were at higher risk for death than those with a below-median HT/infarct size. Left ventricular systolic volume index and HT/infarct size were the strongest predictors of all-cause mortality and cardiovascular mortality in a multivariate analysis. Moreover, HT/infarct size maintained the independent associations with all-cause and cardiovascular mortality after adjusting for age and LVEF.

These studies demonstrated that tissue heterogeneity is present and quantifiable in human infarcts. More extensive tissue heterogeneity correlates with increased ventricular irritability by programmed electrical stimulation and with an increment in cardiac mortality. These findings are consistent with data obtained during voltage

mapping, and show the heterogeneity of the scar in patients with MVT.[28,30]

2.4 3D structure of HT: basis for the differentiation of patients with and without MVT

Recent data obtained from animal and human studies in which scars detected by MRI were imported into navigation systems and merged with electro-anatomical maps have revealed that the MVT substrate is undoubtedly located inside the MRI-detected scar and associated with HT. Ashikaga et al.[37] registered VT activation sequences 10−12 days after infarction with the 3D scar anatomy derived from high-resolution ceMRI. The authors used a porcine model of chronic myocardial infarction based on epicardial sock electrodes or endocardial basket catheters, which are in direct contact with the part of the myocardium where the electrical signal is recorded. MRI revealed a scar with spatially complex structures, particularly at the VT isthmuses. The re-entry isthmus was characterized by a relatively small volume of viable myocardium bound by the scar tissue. Codreanu et al.[38] and Desjardins et al.[39] showed that critical sites of post-infarction MVT arrhythmias were confined to scars detected by voltage mapping that overlapped with areas of high SI. Nevertheless, the MVT substrate inside the scar was not completely characterized in these studies.

In order to gain further insight into the MVT substrate, Perez-David *et al.*[40] compared the architecture of the scar and HT in a group of patients with MVT and in a matched control group. The scar, scar core, and HT were defined as the tissues showing an SI ≥ 2 SD, ≥ 3 SD, and between 2 and 3 SD of remote normal tissue SI, respectively.[35] To determine the architecture of the HT, the authors examined consecutive short-axis slices, in which the HT was automatically coloured based on SI (*Figure 3*). These slices were evaluated to determine the continuity of the HT and its connections to normal myocardium. The HT usually surrounded the core of the scar, but also formed corridor-like structures, through which HT passed from one side to the next by crossing the core of the scar and connecting to normal tissue. These structures are known as HT channels (*Figure 4*). Although no differences were observed regarding LVEF or necrotic mass, HT channels were more common in the MVT group than in the control group (88 vs. 33% of patients; $P < 0.005$). Most HT channels were located partly or totally in the subendocardium.

2.4.1 SI mapping

An SI map is a 3D map in which the average subendocardial or subepicardial SI is projected on a shell that represents either the endocardial or the epicardial surface of the left ventricle. The SI was colour
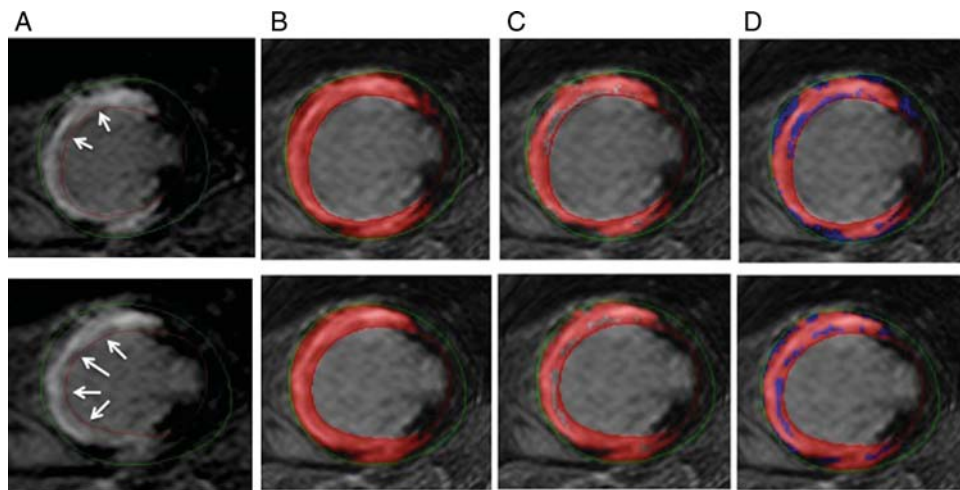

Figure 3 ceMRI characterization of the structure of heterogeneous tissue. Two short-axis slices of an anteroseptal myocardial infarction in a patient from the sustained monomorphic ventricular tachycardia group, showing the following features: (*A*) the unprocessed infarct zone (arrows indicate heterogeneous tissue); (*B*) an area with SI >2 SD; (*C*) an area with signal intensity >3 SD (the core of the scarred area); and (*D*) the differences between (B and C) (SI >2 SD and <3 SD). Heterogeneous tissue is shown in blue. Reproduced with permission from reference 40.
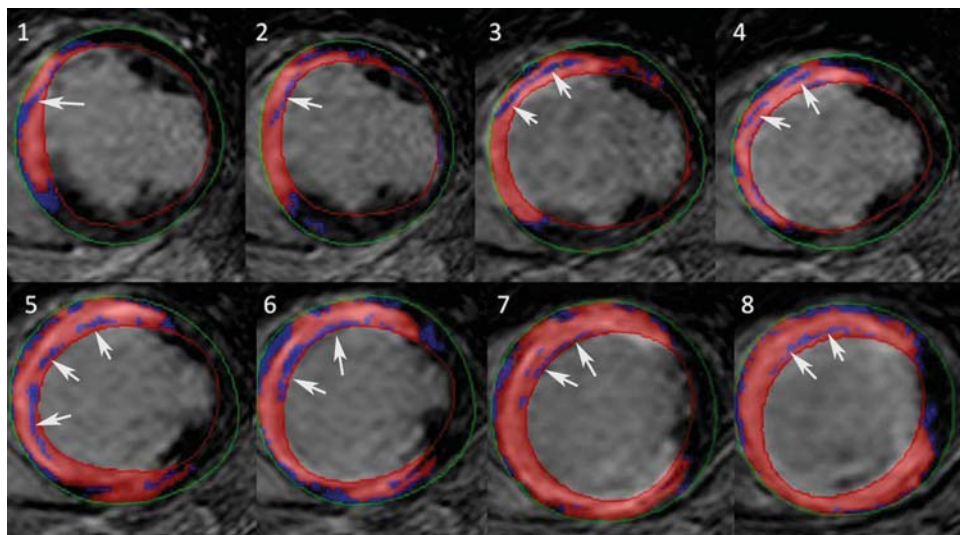

Figure 4 Identification of HT channels. Short-axis slices of a posterolateral myocardial infarction in a patient from the sustained MVT group. Notice the continuity of the HT in the successive short-axis slices, creating a corridor/channel that extends from the base to the apex. White arrows show the HT channel (in blue). Reproduced with permission from reference 40.
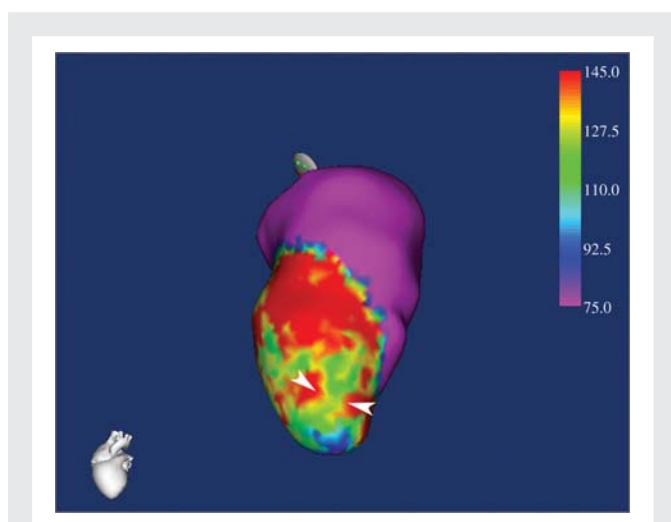
Figure 5 Endocardial SI mapping from a patient with sustained monomorphic ventricular tachycardia (MVT) and an anteroseptal scar. For this process, the left ventricular endocardial/epicardial contours were manually defined on contiguous short-axis slices, which were imported into a custom-developed tool. The average SI of the subendocardial tissue is projected onto the endocardial surface. The colour range provides information on subendocardial SI, as follows: the red area represents an SI > the minimal SI in the core of the scar; the magenta area represents normal myocardium (SI < SI peak in normal myocardium); and the area between these extremes is the heterogeneous tissue.

coded to provide information on the distribution of HT, and to determine the presence of SI channels that were defined as corridors of continuous tissue differentiated by a lower SI from the surrounding scar tissue and connected to normal myocardium via at least one point (*Figure 5*, white arrowheads).

2.4.2 Comparison of voltage and SI mapping in VT patients

The comparison of voltage and SI maps showed a significant relationship between infarct mass (SI > 2 SD) and scar extension defined by < 1.5 mV (R^2, 0.4; $P < 0.009$). SI mapping showed the presence of 26 channels in 17 of 18 patients; these channels coincided in location and orientation with a corresponding CC in the voltage maps (*Figure 6*). Electrograms with IC/LP were recorded in the inner part of all channels. Similar results were recently reported by Andreu et al.,[41] who compared SI and electro-anatomical mapping. Of the 16 CC observed with voltage mapping, 13 (81%) were identified on the 3D ceMRI-derived scar reconstruction when only half of the subendocardial wall was considered. These observations proved the association between IC/LP and HT and, consequently, the association between HT and VT substrate.

2.4.3 Role of SI mapping in the differentiation of patients with and without VT

The information afforded by SI mapping could prove useful for identifying patients at low risk of ventricular arrhythmias.[40] When patients with and without VT were compared, SI channels were more frequently observed in patients with VT. Endocardial SI mapping detected channels in 94% of patients in the sustained MVT group
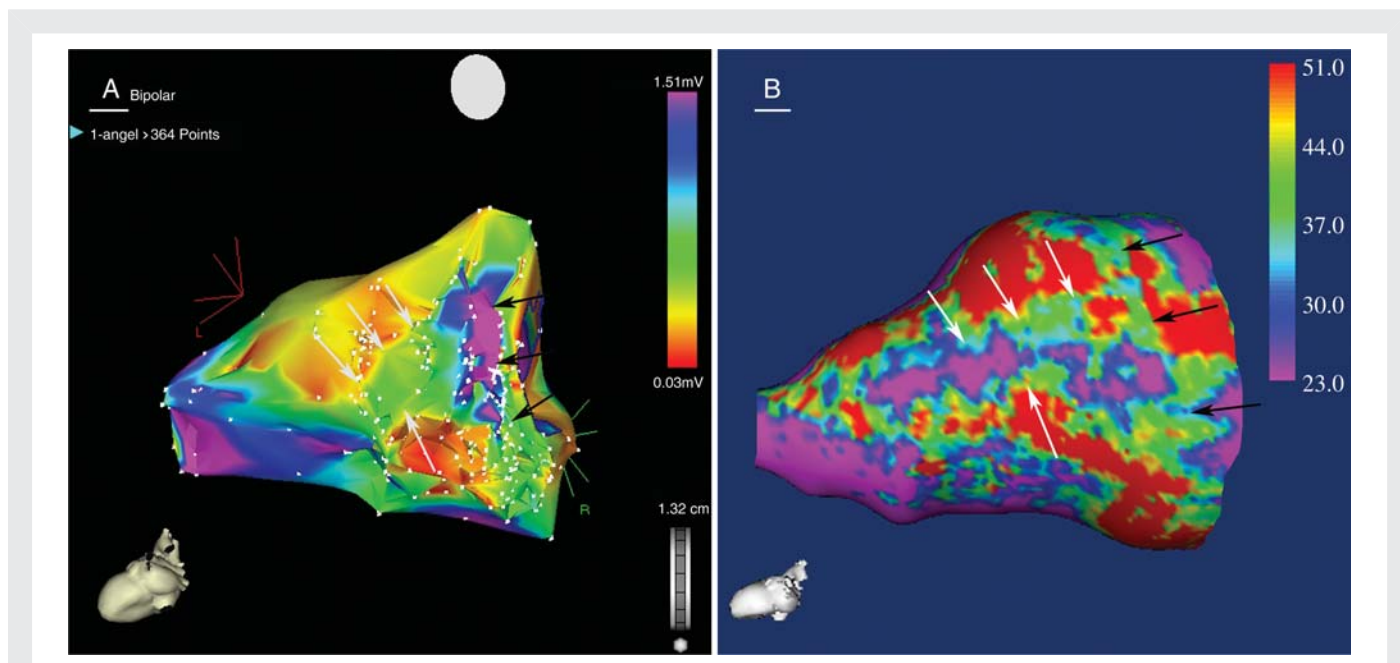

Figure 6 Comparison of voltage and SI mapping. Endocardial voltage (*A*) and SI maps (*B*) from an inferolateral infarction. (A) The voltage map shows the extension of the scar when the voltage scar definition was set between 0.03 and 1.5 mV. Two corridors of higher voltage are easily identified inside the scar. (B) The SI map shows a similar distribution of the scar and a channel that runs parallel to the mitral annulus from segments 6 and 10 (white arrows), and a second channel perpendicular to the mitral annulus between segments 6–8 and 5–7 (black arrows). The colour range provides information on subendocardial SI, as in *Figure 5*. Reproduced with permission from reference 40.

and in only 55% of patients in the control group (*Figure 7*). In addition, complete SI channels, namely, those connected to normal tissue by two sites, were observed in 17 of 18 patients in the VT group, but in only five in the control group. Therefore, the absence of SI channels could enable us to identify low-risk patients, because almost all patients with MVT had SI channels.

2.4.4 Future applications of SI mapping

The ability to quantify HT mass and to determine its structure non-invasively will make it possible to explore and compare new therapeutic strategies that could act on the progression of HT or HT components, such as fibroblasts/myofibroblasts or myocytes. Myocyte division is more intense at the border of the scar,[42] and, when combined with fibroblast proliferation, could influence progression of the VT substrate.[43]

An integrated 3D scar reconstruction from ceMRI may facilitate VT ablations. SI mapping is free from the limitations of voltage mapping, such as poor wall−catheter contact, far-field influences from normal myocardium, or, in the case of epicardial mapping, the presence of epicardial fat. All these limitations could lead to us to underestimate scar dimensions. As SI mapping is free of these limitations, it provides an accurate delimitation of the scar. Although most VT circuits are located in the endocardium, some VTs are only approachable from the epicardium. SI mapping could contribute to the identification of epicardial VT substrate before the electrophysiological study, thus enabling the ablation strategy to be planned before the procedure. Although most patients requiring VT ablations have ICDs, defibrillators are still considered a contraindication for MRI.[44] Although early reports demonstrated potential software and hardware failure, with clinical complications, more recent studies show that ceMRI can be performed safely in selected ICD patients.[45−47] Not

only can MRI be performed safely in patients with ICD, but 3D MRI scar maps can be extracted and registered successfully, and provide important information on complex scar anatomy.[48]

3. VT substrate in non-ischaemic cardiomyopathy

3.1 Scar characteristics in patients with sustained MVT during electro-anatomical mapping

VT in non-ischaemic cardiomyopathy is most commonly the result of myocardial re-entry associated with scar tissue. Soejima *et al.*[49] demonstrated the presence of this mechanism in 22 of 26 patients with monomorphic VT. All patients with myocardial re-entry had endocardial scar tissue (20 of 20 patients) and/or epicardial scar tissue (seven of seven patients mapped). Most scars were adjacent to a valve annulus, and may be greater in extent on the epicardium than on the endocardium. Of the 19 VT circuit isthmuses identified, 12 were associated with an endocardial scar and seven with an epicardial scar.

The results reported by Hsia *et al.* are consistent with the findings presented above.[50] The authors performed left ventricular endocardial electro-anatomical mapping in 19 patients with non-ischaemic cardiomyopathy and MVT. All patients had abnormal low-voltage endocardial areas located near the base of the ventricle in the perivalvular region. Most (88%) of the 57 mapped VTs originated from the base of the ventricle, at sites corresponding to regional scars.

These catheter mapping studies of patients with non-ischaemic cardiomyopathy show the underlying mechanism of VT to be
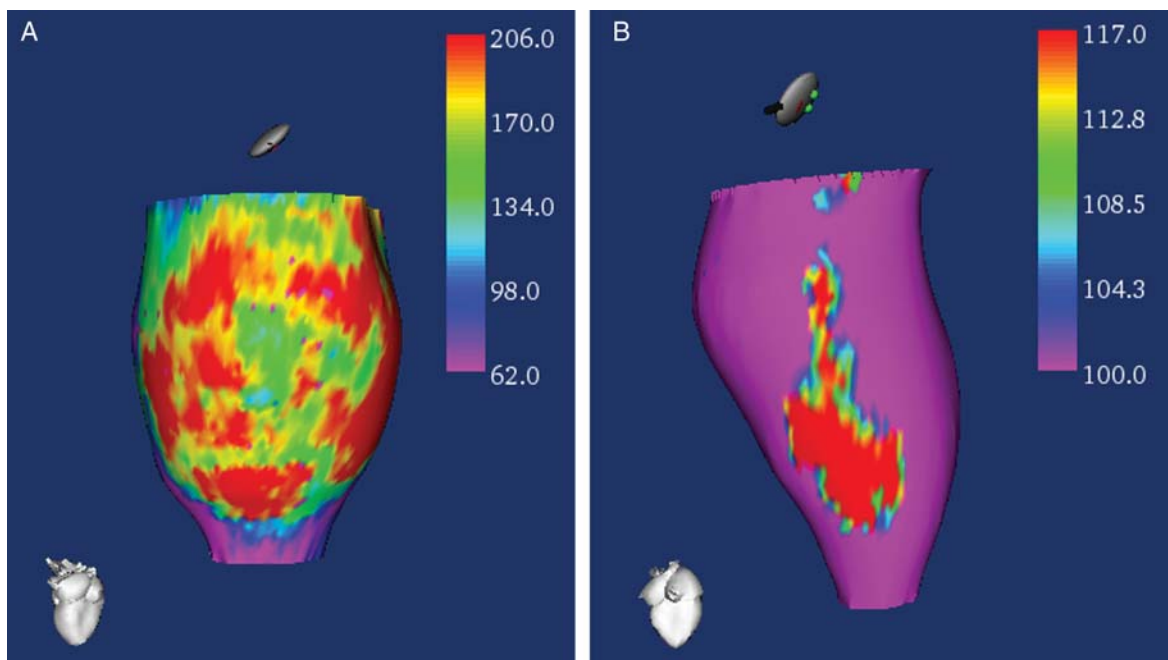

Figure 7 Comparison of SI maps between patients with and without sustained MVT. (*A*) Endocardial SI mapping in a patient with MVT. Notice the presence of multiple SI channels. (*B*) Endocardial SI mapping in a patient from the control group. Notice the absence of SI channels. The colour range provides information on subendocardial SI, as in *Figure 6*.

re-entry around scar tissue deep in the myocardium near the base of the ventricle and in the perivalvular region.

3.2 Characterization of the scar by MRI

Data obtained using ceMRI in patients with an ICD provided similar information to that of voltage mapping in MVT patients. In 26 patients with non-ischaemic cardiomyopathy, the transmural extent of scar tissue as a percentage of wall thickness was calculated in myocardial slices. The predominance of scar tissue involving 26–75% of wall thickness was significantly predictive of inducible VT, and remained independently predictive in the multivariate model after adjustment for LVEF. This study suggested that mid-wall myocardial enhancement involving >25% of wall thickness is the substrate for sustained VT in non-ischaemic cardiomyopathy.[51]

3.2.1 ceMRI and spontaneous VT

Approximately 30% of patients with dilated cardiomyopathy have mid-wall fibrosis, as detected by ceMRI. Regional fibrosis can increase susceptibility to arrhythmia and progression of heart failure. The prognostic implications of mid-wall fibrosis in patients with dilated cardiomyopathy were analysed in a prospective study that included 101 consecutive patients. The fibrosis present in 35% of patients was associated with a higher rate of hospitalization for a cardiovascular condition and total mortality. Multivariate analysis identified mid-wall fibrosis as the sole independent predictor of death or hospitalization. Mid-wall fibrosis was also an independent predictor of sudden cardiac death or VT after correction for baseline differences in LVEF.[52]

Similar results were recently reported by Iles et al.,[53] who prospectively enrolled 103 patients with criteria for primary prevention of sudden cardiac death. ceMRI was performed before placement of the ICD, and identified regional fibrosis in 51% of patients with non-ischaemic cardiomyopathy and in all 42 patients with ischaemic cardiomyopathy. There was a 14% discharge rate in the ischaemic cardiomyopathy group (six of 42). Although no ICD discharges were observed in the non-ischaemic cardiomyopathy group without regional fibrosis, 29% of patients with regional fibrosis received ICD shocks. The LVEF was similar in patients with and without device therapy (24 ± 12 vs. 26 ± 8%, $P = NS$) and those with or without regional fibrosis (25 ± 9 vs. 26 ± 9%, $P = NS$).

4. Conclusions

HT is a consequence of the remodelling process, in which surviving myocytes, fibroblasts/myofibroblasts, and the extracellular matrix interact mechanically and electrically to form the VT substrate. ceMRI makes it possible to determine the size and 3D structure of the scar and HT. This information could be useful when evaluating new therapies focused on the control of remodelling processes and risk stratification in patients with structural heart disease.

5. Clinical implication

Non-invasive identification and characterization of VT substrate could facilitate the identification of patients at risk of ventricular arrhythmias. This information should be assessed in large multicentre studies and compared with other predictors of cardiac mortality, such as functional and volume parameters of the left ventricle. Screening of patients for primary prevention of sudden cardiac death could be improved by the analysis of the scar characteritics. In addition, non-

invasive identification of VT substrate could improve the ablation procedure.

References

1. De Bakker JM, van Capelle FJ, Janse MJ, Wilde AA, Coronel R, Becker AE et al. Reentry as a cause of VT in patients with chronic ischemic heart disease: electrophysiologic and anatomic correlation. Circulation 1988;**77**:589–606.
2. Yousef ZR, Redwood SR, Marber MS. Postinfarction left ventricular remodelling: where are the theories and trials leading us? Heart 2000;**83**:76–80.
3. De Bakker J, Coronel R, Tasseron S, Wilde AA, Opthof T, Janse MJ et al. Ventricular tachycardia in the infarcted Langendorff-perfused human heart: role of the arrangement of surviving cardiac fibres. J Am Coll Cardiol 1990;**15**:1594–1607.
4. De Bakker J, Van Capelle F, Janse M, Tasseron S, Vermeulen JT, de Jonge N et al. Slow conduction in the infarcted human heart: zigzag course of activation. Circulation 1993;**88**:915–926.
5. Saffitz JE, Schuessler RB, Yamada KA. Mechanisms of remodeling of gap junction distributions and the development of anatomic substrates of arrhythmias. Cardiovasc Res 1999;**42**:309–317.
6. Beardslee MA, Laing JG, Beyer EC, Saffitz JE. Rapid turnover of connexin43 in the adult rat heart. Circ Res 1998;**83**:629–635.
7. Kieken F, Mutsaers N, Dolmatova E, Virgil K, Wit AL, Kellezi A et al. Structural and molecular mechanisms of gap junction remodeling in epicardial border zone myocytes following myocardial infarction. Circ Res 2009;**104**:1103–1112.
8. Van Rijen HVM, Eckardt D, Degen J, Theis M, Ott T, Willecke K et al. Slow conduction and enhanced anisotropy increase the propensity for ventricular tachyarrhythmias in adult mice with induced deletion of connexin43. Circulation 2004;**109**:1048–1055.
9. Van Veen TAB, Stein M, Royer A, Quang KL, Charpentier F, Colledge WH et al. Impaired impulse propagation in Scn5a-knockout mice: combined contribution of excitability, connexin expression, and tissue architecture in relation to aging. Circulation 2005;**112**:1927–1935.
10. Camelliti P, Borg TK, Kohl P. Structural and functional characterization of cardiac fibroblasts. Cardiovasc Res 2005;**65**:40–51.
11. Kanekar S, Hirozanne T, Terracio L, Borg TK. Cardiac fibroblasts: form and function. Cardiovasc Pathol 1998;**7**:127–133.
12. Souders CA, Bowers SLK, Baudino TA. Cardiac fibroblast: the renaissance cell. Circ Res 2009;**105**:1164–1176.
13. Louault C, Benamer N, Faivre JF, Potreau D, Bescond J. Implication of connexins 40 and 43 in functional coupling between mouse cardiac fibroblasts in primary culture. Biochim Biophys Acta 2008;**1778**:2097–2104.
14. Kohl P. Heterogeneous cell coupling in the heart: an electrophysiological role for fibroblasts. Circ Res 2003;**93**:381–383.
15. Spach MS, Boineau JP. Microfibrosis produces electrical load variations due to loss of side-to-side cell connections: a major mechanism of structural heart disease arrhythmias. Pacing Clin Electrophysiol 1997;**20**:397–413.
16. Gabbiani G. The cellular derivation and the life span of the myofibroblast. Pathol Res Pract 1996;**192**:708–711.
17. Vasquez C, Mohandas P, Louie KL, Benamer N, Bapat AC, Morley GE. Enhanced fibroblast–myocyte interactions in response to cardiac injury. Circ Res 2010;**107**:1011–1020.
18. DeMaziere AMGL, VanGinneken ACG, Wilders R, Jongsma HJ, Bouman LN. Spatial and functional relationship between myocytes and fibroblasts in the rabbit sinoatrial node. J Mol Cell Cardiol 1992;**24**:567–578.
19. Willems IE, Havenith MG, De Mey JG, Daemen MJ. The alpha-smooth muscle actin-positive cells in healing human myocardial scars. Am J Pathol 1994;**145**:868–875.
20. Gaudesius G, Miragoli M, Thomas SP, Rohr S. Coupling of cardiac electrical activity over extended distances by fibroblasts of cardiac origin. Circ Res 2003;**93**:421–428.
21. Miragoli M, Gaudesius G, Rohr S. Electrotonic modulation of cardiac impulse conduction by myofibroblasts. Circ Res 2006;**98**:801–810.
22. Thompson SA, Copeland CR, Reich DH, Tung L. Mechanical coupling between myofibroblasts and cardiomyocytes slows electric conduction in fibrotic cell monolayers. Circulation 2011;**123**:2083–2093.
23. Josephson ME. Clinical Cardiac Electrophysiology. 3rd ed. Philadelphia: Lippincott Williams & Wilkins; 2002.

24. Callans DJ, Ren JF, Michele J, Marchlinski FE, Dillon SM. Electroanatomic left ventricular mapping in the porcine model of healed anterior myocardial infarction: correlation with intracardiac echocardiography and pathological analysis. *Circulation* 1999;**100**: 1744–1750.

25. Marchlinski FE, Callans DJ, Gottlieb CD, Zado E. Linear ablation lesions for control of unmappable ventricular tachycardia in patients with ischemic and nonischemic cardiomyopathy. *Circulation* 2000;**101**:1288–1296.

26. Arenal A, Glez-Torrecilla E, Ortiz M, Villacastin J, Fdez-Portales J, Sousa E *et al.* Ablation of electrograms with an isolated, delayed component as treatment of unmappable monomorphic ventricular tachycardias in patients with structural heart disease. *J Am Coll Cardiol* 2003;**41**:81–92.

27. Bogun F, Good E, Reich S, Elmouchi D, Igic P, Lemola K *et al.* Isolated potentials during sinus rhythm and pace-mapping within scars as guides for ablation of post-infarction ventricular tachycardia. *J Am Coll Cardiol* 2006;**47**:2013–2019.

28. Arenal A, del Castillo S, Gonzalez-Torrecilla E, Atienza F, Ortiz M, Jimenez J *et al.* Tachycardia-related channel in the scar tissue in patients with sustained monomorphic ventricular tachycardias: influence of the voltage scar definition. *Circulation* 2004; **110**:2568–2574.

29. Hsia HH, Lin D, Sauer WH, Callans DJ, Marchlinski FE. Anatomic characterization of endocardial substrate for hemodynamically stable reentrant ventricular tachycardia: identification of endocardial conducting channels. *Heart Rhythm* 2006;**3**:503–512.

30. Nakahara S, Tung R, Ramirez RJ, Gima J, Wiener I, Mahajan A *et al.* Distribution of late potentials within infarct scars assessed by ultra high-density mapping. *Heart Rhythm* 2010;**7**:1817–1824.

31. Crawford T, Cowger J, Desjardins B, Kim HM, Good E, Jongnarangsin K *et al.* Determinants of postinfarction ventricular tachycardia. *Circ Arrhythm Electrophysiol* 2010;**3**: 624–631.

32. Haqqani HM, Kalman JM, Roberts-Thomson KC. Fundamental differences in electrophysiologic and electroanatomic substrate between ischemic cardiomyopathy patients with and without clinical ventricular tachycardia. *J Am Coll Cardiol* 2009;**54**: 166–173.

33. Amado LC, Gerber BL, Gupta SN, Rettmann DW, Szarf G, Schock R *et al.* Accurate and objective infarct sizing by contrast-enhanced magnetic resonance imaging in a canine myocardial infarction model. *J Am Coll Cardiol* 2004;**44**:2383–2389.

34. Bello D, Fieno DS, Kim RJ, Pereles FS, Passman R, Song G *et al.* Infarct morphology identifies patients with substrate for sustained ventricular tachycardia. *J Am Coll Cardiol* 2005;**45**:1104–1108.

35. Yan AT, Shayne AJ, Brown KA, Gupta SN, Chan CW, Luu TM *et al.* Characterization of the peri-infarct zone by contrast-enhanced cardiac magnetic resonance imaging is a powerful predictor of post-myocardial infarction mortality. *Circulation* 2006;**114**: 32–39.

36. Schmidt A, Azevedo CF, Cheng A, Gupta SN, Bluemke DA, Foo TK *et al.* Infarct tissue heterogeneity by magnetic resonance imaging identifies enhanced cardiac arrhythmia susceptibility in patients with left ventricular dysfunction. *Circulation* 2007;**115**: 2006–2014.

37. Ashikaga H, Sasano T, Dong J, Zviman MM, Evers R, Hopenfeld B *et al.* Magnetic resonance-based anatomical analysis of scar-related ventricular tachycardia: implications for catheter ablation. *Circ Res* 2007;**101**:939–947.

38. Codreanu A, Odille F, Aliot E, Marie PY, Magnin-Poull I, Andronache M *et al.* Electroanatomic characterization of post-infarct scars: comparison with 3-dimensional myocardial scar reconstruction based on magnetic resonance imaging. *J Am Coll Cardiol* 2008;**52**:839–842.

39. Desjardins B, Crawford T, Good E, Oral H, Chugh A, Pelosi F *et al.* Infarct architecture and characteristics on delayed enhanced magnetic resonance imaging and electroanatomic mapping in patients with postinfarction ventricular arrhythmia. *Heart Rhythm* 2009;**6**:644–651.

40. Perez-David E, Arenal Á, Rubio-Guivernau JL, del Castillo R, Atea L, Arbelo E *et al.* Noninvasive identification of ventricular tachycardia-related conducting channels using contrast-enhanced magnetic resonance imaging in patients with chronic myocardial infarction: comparison of signal intensity scar mapping and endocardial voltage mapping. *J Am Coll Cardiol* 2011;**57**:184–194.

41. Andreu D, Berruezo A, Ortiz-Pérez JT, Silva E, Mont L, Borràs R *et al.* Integration of 3D electroanatomic maps and magnetic resonance scar characterization into the navigation system to guide ventricular tachycardia ablation. *Circ Arrhythm Electrophysiol* 2011;**4**:674–683.

42. Beltrami AP, Urbanek K, Kajstura J, Yan SM, Finato N, Bussani R *et al.* Evidence that human cardiac myocytes divide after myocardial infarction. *N Engl J Med* 2001;**344**: 1750–1757.

43. Bogun F, Krishnan S, Siddiqui M, Good E, Marine JE, Schuger C *et al.* Electrogram characteristics in postinfarction ventricular tachycardia. Effect of infarct age. *J Am Coll Cardiol* 2005;**46**:667–674.

44. Faris OP, Shein M. Food and Drug Administration perspective: magnetic resonance imaging of pacemaker and implantable cardioverter-defibrillator patients. *Circulation* 2006;**114**:1232–1233.

45. Gimbel JR, Kanal E, Schwartz KM, Wilkoff BL. Outcome of magnetic resonance imaging (MRI) in selected patients with implantable cardioverter defibrillators (ICDs). *Pacing Clin Electrophysiol* 2005;**28**:270–273.

46. Naehle CP, Strach K, Thomas D, Meyer C, Linhart M, Bitaraf S *et al.* Magnetic resonance imaging at 1.5-T in patients with implantable cardioverter-defibrillators. *J Am Coll Cardiol* 2009;**54**:549–555.

47. Nazarian S, Roguin A, Zviman MM, Lardo AC, Dickfeld TL, Calkins H *et al.* Clinical utility and safety of a protocol for noncardiac and cardiac magnetic resonance imaging of patients with permanent pacemakers and implantable cardioverter defibrillators at 1.5 Tesla. *Circulation* 2006;**114**:1277–1284.

48. Dickfeld T, Tian J, Ahmad G, Jimenez A, Turgeman A, Kuk R *et al.* MRI-guided ventricular tachycardia ablation: integration of late gadolinium-enhanced 3D scar in patients with ICD. *Circ Arrhythm Electrophysiol* 2011;**4**:172–184.

49. Soejima K, Stevenson WG, Sapp JL, Selwyn AP, Couper G, Epstein LM. Endocardial and epicardial radiofrequency ablation of ventricular tachycardia associated with dilated cardiomyopathy: the importance of low-voltage scars. *J Am Coll Cardiol* 2004;**43**:1834–1842.

50. Hsia HH, Callans DJ, Marchlinski FE. Characterization of endocardial electrophysiological substrate in patients with nonischemic cardiomyopathy and monomorphic ventricular tachycardia. *Circulation* 2003;**108**:704–710.

51. Nazarian S, Bluemke DA, Lardo AC, Zviman MM, Watkins SP, Dickfeld TL *et al.* Magnetic resonance assessment of the substrate for inducible ventricular tachycardia in nonischemic cardiomyopathy. *Circulation* 2005;**112**:2821–2825.

52. Assomull RG, Prasad SK, Lyne J, Smith G, Burman ED, Khan M *et al.* Cardiovascular magnetic resonance, fibrosis, and prognosis in dilated cardiomyopathy. *J Am Coll Cardiol* 2006;**48**:1977–1985.

53. Iles L, Pfluger H, Lefkovits L, Butler MJ, Kistler PM, Kaye DM *et al.* Myocardial fibrosis predicts appropriate device therapy in patients with implantable cardioverter-defibrillators for primary prevention of sudden cardiac death. *J Am Coll Cardiol* 2011;**57**:821–828.